

Nucleobase-Modified Microgels Synthesized via Microfabrication Technology for DNA Adsorption

Kemal Cetin^{1,2} 

¹ Necmettin Erbakan University, Faculty of Engineering, Department of Biomedical Engineering, Konya, Türkiye.

² Necmettin Erbakan University, Science and Technology Research and Application Center (BITAM), Konya, Türkiye.

ABSTRACT

DNA isolation is a crucial procedure since DNA-based assays have great importance in molecular biology, biochemistry and biomedical applications. The objective of this study is to fabricate micron-sized hydrogels as adsorbents for DNA. Poly(2-hydroxyethyl methacrylate-co-glycidyl methacrylate) microgels were synthesized by free radical polymerization in the presence of N,N'-methylenebisacrylamide as a crosslinker, in the microholes of a microstencil array chip. Then, adenine was immobilized to microgels through the epoxy groups of glycidyl methacrylate. Scanning electron microscopy and Fourier transform infrared spectroscopy were employed to investigate the chemical and morphological characterizations of the microgels. The findings of the experiments demonstrate that the microgels had a cylindrical shape, were of uniform size, and had a height and diameter of around 500 µm. Observation of aromatic C=C peak confirmed the existence of adenine ligand in the microgel structure. Adsorption studies were carried out to determine the optimal conditions for DNA adsorption of nucleobase-immobilized microgels. After initially increasing, the quantity of DNA adsorbed onto the microgels reached a saturation level at a DNA concentration of around 2.0 mg/mL. The maximum adsorption was 38.54 mg/g microgels for an initial DNA concentration of 2.0 mg/mL in the optimum medium pH and temperature. DNA adsorption capabilities are shown to not significantly decline in recurrent adsorption-desorption cycles. As a result of the findings, adenine-immobilized microgels were demonstrated to be a viable option for DNA adsorption. Additionally, as a reference for future research, this study highlights the benefits of microfabrication technology, such as its simplicity of use in fabricating adsorption materials with the desired size, shape, and uniformity.

Keywords:

Adsorption; DNA; Hydrogels; Microfabrication; Microgels; Nucleobase

INTRODUCTION

DNA isolation/extraction from biological samples is a fundamental and significant process in biochemistry, molecular biology, forensics, clinical analysis, and DNA-based biomedical applications [1–3]. DNA isolation has great potential usage in gene therapy, the treatment of autoimmune diseases, DNA vaccination, pathogen detection, biosensor applications and so on [2,4–6]. The importance of DNA and DNA isolation has made it crucial to develop DNA isolation procedures and techniques. The need for innovative methods is demonstrated by the fact that conventional ones need time-consuming steps like centrifugation and precipitation as well as the usage of harmful chemicals for both the environment and human health [7].

Hydrogels are polymeric structures with a high-water retention capacity in their 3D matrices. They are insoluble in water due to their physically or/and chemically cross-linked structure, but instead, exhibit high swelling capacity [8,9]. Because of their promising properties, hydrogels have been used in various applications in biochemistry, biotechnology, and biomedical engineering. For example, they can be used in tissue engineering owing to their tissue-like swelling properties and biocompatibility, in drug delivery systems because of their ability to load the desired amount of drug and injectable formulation, and in affinity chromatography for the separation of biomolecules like proteins due to allowing modifications such as ligand immobilization of the polymer matrix [10–12].

Article History:

Received: 2023/06/06

Accepted: 2023/10/12

Online: 2023/12/31

Correspondence to: Kemal Çetin,
kccetin@erbakan.edu.tr

This article has been checked for similarity.



This is an open access article
under the CC-BY-NC licence

<http://creativecommons.org/licenses/by-nc/4.0/>

Cite as:

K. CETIN, "Nucleobase-Modified Microgels Synthesized via Microfabrication Technology for DNA Adsorption" *Hittite Journal of Science and Engineering*, vol. 10, no. 4, pp. 309–315, 2023. doi:10.17350/hjse19030000320

Microfabrication processes have been widely employed in electronics and bioelectronics in order to fabricate micro-electro-mechanical systems (MEMS) including sensors, cantilevers, microreservoirs, micropumps, rotors, channels, valves, and so on [13]. Besides electronics, micro- and nano-fabrication methods are potentially powerful tools to improve devices in biotechnology and biochemical processing, such as miniaturized chromatography systems, lab-on-a-chip devices, and microreactors [14,15]. Microengineered hydrogels, one of the significant products of microfabrication, have great potential in tissue engineering and drug delivery systems due to their abilities of mimicking the physical, mechanical, and biological features of natural tissues and organs [16–18].

Recently, Wu et al. studied the effect of metal ions such as Na^+ , Mg^{2+} , Ca^{2+} , Mn^{2+} and Zn^{2+} on the adsorption of both single-stranded DNA (ssDNA) and double-stranded DNA (dsDNA) onto microplastics and they reported that the transition metals, i.e., Mn^{2+} and Zn^{2+} , showed a higher adsorption capacity than Mg^{2+} for both dsDNA and ssDNA [19]. For DNA extraction and amplification, Wang et al. immobilized Ti^{4+} on magnetic composite microspheres and reported the extraction ability as $84 \pm 4 \mu\text{g}/\text{mg}$ [20]. By polymerizing HEMA with N-methacryloyl-L-tryptophan which is a hydrophobic ligand, Çorman et al. synthesized two different types of hydrophobic cryogels: the first is poly(2-hydroxyethyl methacrylate-N-methacryloyl-L-tryptophan) [P(HEMA-MATrp)] cryogel, and the second is P(HEMA-MATrp) particles embedded PHEMA cryogel [21]. Maximum adsorption of DNA on p(HEMA-MATrp) cryogel and p(HEMA-MATrp) embedded PHEMA composite cryogel were found to be 15 mg/g and 38 mg/g polymer, respectively. The results showed that embedding hydrophobic micro-particles showed higher adsorption capacity compared to hydrophobic cryogels [21]. Zandieh et al. studied on adsorption of DNA oligonucleotides onto microplastics in the absence and presence of metal ions and reported that polyethylene terephthalate and polystyrene showed the highest DNA adsorption efficiency [22]. Wang et al. prepared self-assembled zinc meso-tetra(4-pyridyl)porphyrin for DNA adsorption and adsorption of single-stranded DNA showed higher efficiency compared to duplex DNA [23]. In another study, Meng et al. developed a biosensor based on adsorption of DNA on polydopamine nanoparticles via different metal ions including Na^+ , K^+ , Mg^{2+} and Ca^{2+} coordination and detection limit in various biological samples including serum was provided as $<1 \text{ nM}$ target DNA [24]. Muñoz et al. investigated the effect of homonuclear boron bonds on the adsorption of DNA nucleobases using quantum-mechanics calculations and concluded that the adsorption is improved by homonuclear bonds in the boron nitride nanosheets [25].

In this study, microfabrication technology was used to

synthesize micro-engineered hydrogels, i.e., microgels with a height and diameter of around $500 \mu\text{m}$. Microgels were produced in the microholes of a microstencil array chip (MAC) by free-radical polymerization of 2-hydroxyethyl methacrylate (HEMA) and glycidyl methacrylate (GMA) while N, N'-methylenebisacrylamide (MBA) was employed as a crosslinker. Investigating the effects of medium pH, initial DNA concentration, adsorption time, and ambient temperature on the adsorption capacity of microgels allowed for the identification of the optimal DNA adsorption conditions.

MATERIAL AND METHODS

Materials

HEMA, DNA (D3159, from herring sperm), GMA, ammonium persulfate (APS), MBA, and N,N,N',N'-tetramethyl ethylene diamine were purchased from Sigma Chemical Co. (St. Louis, MO, USA). Direct-Q 3 UV; Merck Millipore, Burlington, MA, USA system provided deionized water (DI Water) throughout the duration of the experimental research.

Fabrication of Microgels

Microgels prepared with the aid of a MAC are described as follows: Firstly, MBA (0.1% w/v) was dissolved in deionized (DI) water. HEMA:GMA ratio was adapted from an earlier study [26]. After adding HEMA (2.25 mL) and GMA (0.50 mL) to the MBA solution, it was magnetically stirred for 15 min. After APS (28.96 mg) was dissolved in the mixture, TEMED (11.4 μL) was added. Following the addition of ethanol (4 mL), the solutions were stirred once more and nitrogen bubbled for 5 min. The mixture was carefully put on a MAC. After 3 hours of polymerization at 60°C , it was terminated at 4°C , and microgels were collected.

Immobilization of Adenine onto Microgels

0.1 M of adenine solution was prepared in DI water : dioxane (1:1 v/v) and microgels were added into this mixture then the immobilization reaction was performed at 80°C by shaking for 24 h [27].

Characterization Studies

Prior to the Attenuated Total Reflection–Fourier Transform Infrared (ATR–FTIR) analysis, microgels were firstly freeze-dried at -110°C for 24 h in a freeze-drying unit (Labogene Coolsafe Touch, Denmark). Using a Thermo Scientific Nicolet iS20 FTIR-ATR spectrophotometer (USA), FTIR spectra of the microgels were obtained in the wavelength range from 4000 to 500 cm^{-1} through 32 repeated scans at a 4 cm^{-1} resolution. Before the sample test, background measurements were made, which were automatically subtracted from the sample re-

sults. The overall shape and dimensions of the freeze-dried microgels were examined using an optical microscope (Olympus SZ6, Japan). To discuss the morphology of the microgels, a ZEISS GeminiSEM 500 field emission scanning electron microscope (FE-SEM) (Germany) was used.

Adsorption Studies

DNA adsorption capability of microgels was investigated in a batch experiment setup. The following conditions were studied to determine the optimal conditions for DNA adsorption of the microgels. The effects of medium pH (4-9) and temperature (4-45 °C), as well as the effects of initial DNA concentration (0.25-4.0 mg/mL) and adsorption time (2.5-60 min) on DNA adsorption capacity of microgels were investigated. DNA concentrations were determined at 260 nm using a UV-visible spectrophotometer and the amount of adsorbed DNA was evaluated via the Equation 1:

$$Q = \frac{(c_0 - c_f)v}{w} \quad (1)$$

where Q (mg/g dry microgel) is the adsorption capacity. The initial and final concentrations of DNA (in mg/mL) are shown by the symbols C_0 and C_f before and after the adsorption process, respectively. W is the dried microgel mass in g, and V is the volume of the DNA solution in mL.

RESULTS AND DISCUSSION

General shape and size of the microgels were evaluated via optical microscopy. As shown in Fig.1, microgels exhibit cylindrical shapes with the highest size of around 400–500 μm. Surface morphology of the microgels were revealed using FE-SEM as shown in Fig. 2. Microgels exhibit, in general, homogenous porous microstructure.

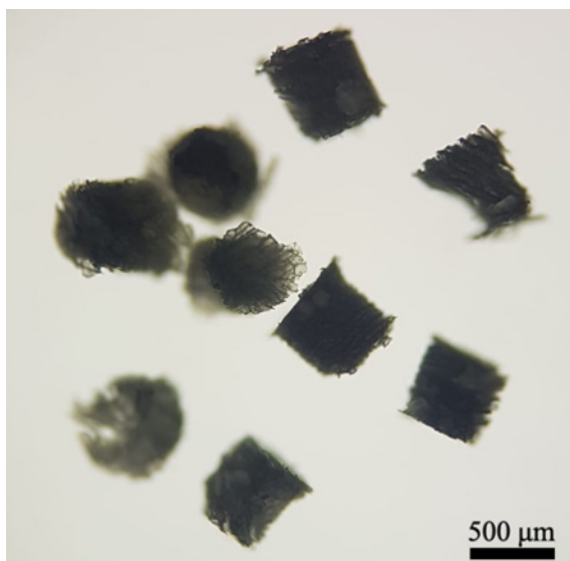


Figure 1. Optical microscopy images of the microgels

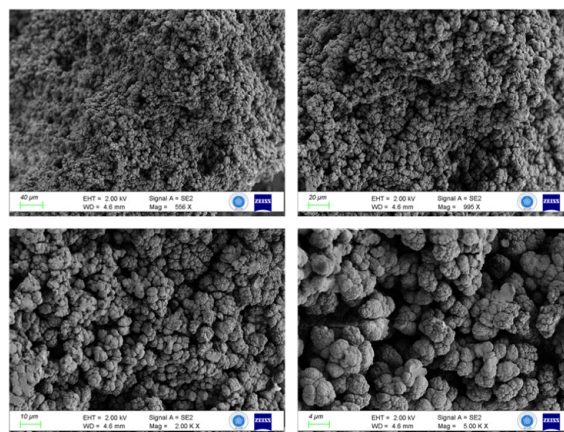


Figure 2. FE-SEM images of the microgels

We employed the Fourier transform infrared (FT-IR) spectroscopy approach to analyze the chemical composition of both plain and immobilized microgels (Fig. 3). The common bands were given at about 3400 cm^{-1} , 1710 cm^{-1} , and 2968 and 2946 cm^{-1} , respectively, for the -OH, C-H (aliphatic) and C=O bonds [26]. The C=C peaks at 1637 cm^{-1} have relatively low intensities, which supports polymerization.

The almost absence of C=C peaks around 1630 cm^{-1} confirms the polymerization [28]. Besides these, aromatic C=C peak indicates the existence of adenine ligand.

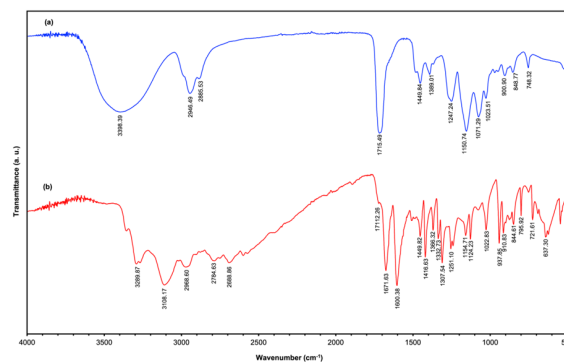


Figure 3. FT-IR spectra of the (a) P(HEMA-GMA) and (b) P(HEMA-GMA)-Adenine microgels

Fig. 4 depicts how medium pH affects the adsorption of DNA by the microgels. At pH 7.0, the adsorption capacity was at its maximum while declined at more alkaline and more acidic pH regions. Decrements in adsorption capacities were observed for pH 4.0 and pH 9.0 by about 18% and 23%, respectively, compared to the one in pH 7.0. This indicates that the interaction between adenine and thymine was weakened in acidic and basic environments by the presence of hydronium or hydroxy ions [29].

Fig. 5 presents the effect of adsorption time on the DNA adsorption by the microgels. Although the rate of DNA ad-

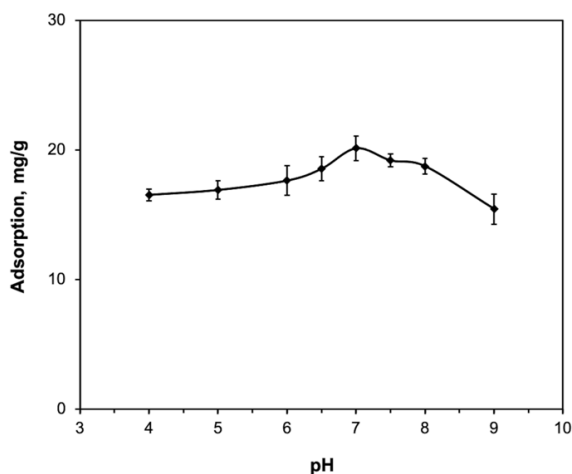


Figure 4. The adsorbed amount of DNA at various pH values (Temperature: 25 °C; initial DNA concentration: 0.5 mg/mL)

sorption was initially high, it started to decline after only 2.5 min, and equilibrium adsorption was attained upto 5 min. As a result, for the optimal adsorption capacity, ligand and analyte molecules need a short interaction time. It is clear that the interaction between DNA molecules and microgels had a high affinity since microgels might reach their maximum adsorption capacity in just 5 min. This is mostly due to the fact that microgels include adenine molecules as ligands, which is consistent with the literature [7]. Additionally, DNA molecules can quickly reach and interact with the active regions of the gel matrix because of the hydrophilic nature of hydrogels [30].

As it is seen in Fig. 6, there was an increment in the adsorption capacity as the initial concentration of DNA increased. At an initial DNA concentration of 0.5 mg/L, the adsorption capacity of microgels was 20.18 mg/g, whereas, at an initial DNA concentration of 1.0 mg/mL, it reached up to 38.54 mg/g. At a DNA concentration of around 2.0 mg/L, the adsorption process approached a plateau level, i.e., 38.54

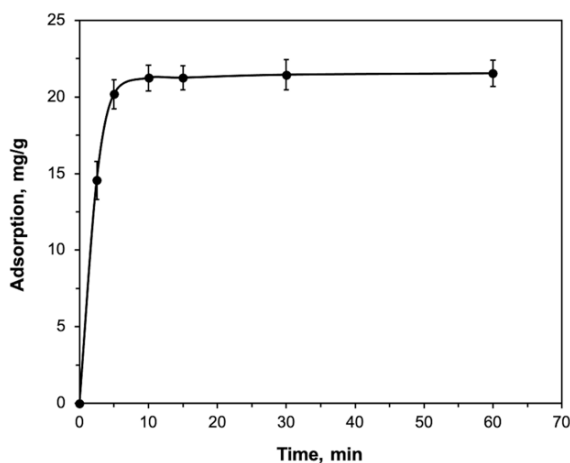


Figure 5. The adsorbed amount of DNA at various adsorption time (Running buffer: pH 7.0 phosphate; temperature: 25 °C; initial DNA concentration: 0.5 mg/mL)

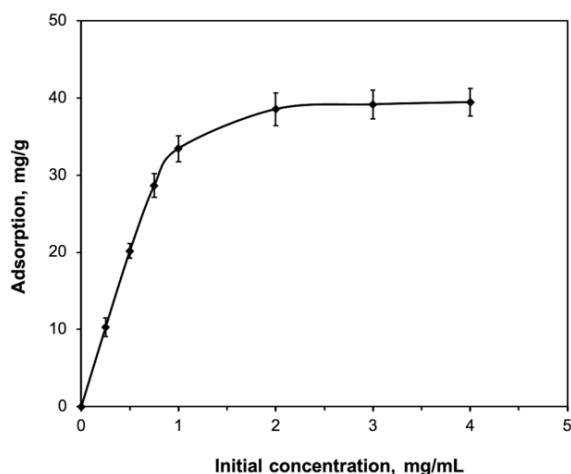


Figure 6. The adsorbed amount of DNA at various DNA concentrations (Running buffer: pH 7.0 phosphate; temperature: 25 °C)

mg/g. Even if the initial concentration value of DNA was exceeded, DNA adsorption has reached a dynamic equilibrium value because all active adenine ligands in the microgels were occupied with analyte molecules, i.e. DNA. Similar results have been observed in previous DNA adsorption studies [24,31,32].

As shown in Fig. 7, it can be observed that the adsorption capacity slightly increased as the temperature raised. One possible explanation is that as the temperature increased, the DNA double helix structure may partially expanded, facilitating easier interaction between the ligand and nucleotides [7].

A comparison of the adsorption capacity and duration of adsorption process of the microfabricated microgels with those of some other adsorbents reported in literature is listed in Table 1. Considering the fast kinetics of the DNA adsorption of the microgels, it is predicted that these newly designed microgels may be a good alternative in DNA adsorption.

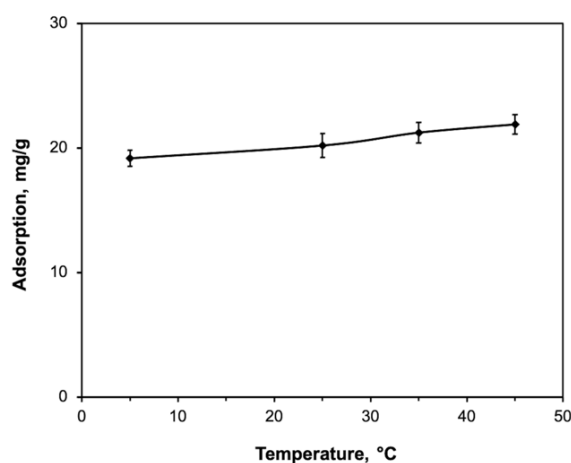


Figure 7. The adsorbed amount of DNA at various temperature values (Running buffer: pH 7.0 phosphate; initial DNA concentration: 0.5 mg/mL)

Table 1. Comparison of the DNA adsorption capacities of numerous adsorbents.

Adsorbent	Adsorption capacity	Adsorption time (min)	Ref.
Hemoglobin modified magnetic nanocomposites (NCs)	27.9 mg/g	15	[1]
Co(II) immobilized poly(GMA-EDMA) cryogels	33.81 mg/g	30	[5]
Aminosilane-modified magnetic nanoparticles (NPs)	4.7 mg/g	40	[33]
Ethylenediamine functionalized poly(glycidyl methacrylate) beads	90.4 µg/g	-	[34]
P(HEMA-(l)-histidine methyl ester)	13.5 mg/g	-	[35]
Silica-magnetite NCs	43.1 mg/g	8	[36]
Triethylamine modified poly(GMA-EDMA) monoliths	21.54 mg/mL	-	[37]
Cibacron Blue F3GA-attached poly(hydroxyethyl methacrylate)	32.5 mg/g	120	[38]
Zirconia magnetic NCs	53.5 mg/g	5	[39]
Magnetic polyaniline/maghemite NCs	75.2 mg/g	10	[40]
P(HEMA-MATrp) cryogels	3.53 mg/g	60	[21]
P(HEMA-MATrp) microbeads in PHEMA cryogels	8.35 mg/g	60	[21]
Composite cryogels of cyanobacterial extracellular polymeric substances and PHEMA	2.4 mg/g	-	[41]
Fe ²⁺ ions attached EPS-PHEMA composite cryogels	39.7 mg/g	-	[41]
Cu ²⁺ -attached magnetite NPs embedded PHEMA cryogels	19.97 mg/g	120	[42]
16mer peptide modified poly(EDMA-GMA)	65.1 µg/g	5	[43]
Indium Tin Oxide NPs	28.5 nM	120	[44]
Magnetic Mesoporous Silica NPs	121.6 mg/g	>20 h	[45]
Microfabricated nucleobase-modified microgels	38.54 mg/g	10	This study

While a material's capacity to be reused has economic benefits, it is also vital to reducing the usage of single-use plastics from polluting the environment [46]. For this objective, the adsorption capabilities of the synthesized microgels were evaluated for their not only single-use but also repeated-use effects on DNA adsorption capability. Figure 8 illustrates how the adsorption capacity of the same microgels decreased after each use in comparison to the prior capacity. During the adsorption-desorption cycle, a decrease in the adsorption capacity of the adsorbent may be observed for various reasons including loss in the active site for the analyte molecules due to tear and/or wear in the adsorbent, precipitation on the adsorbent surface, low desorption ef-

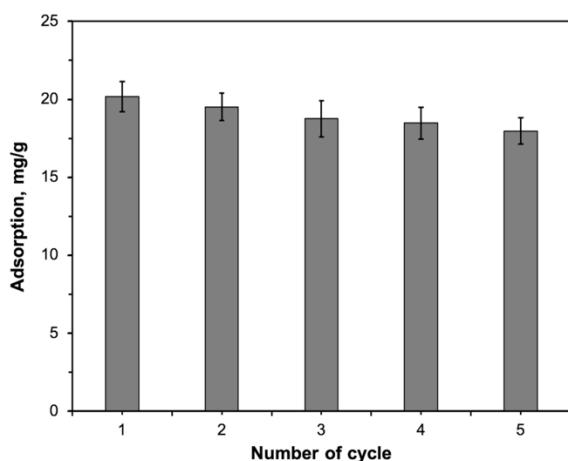


Figure 8. Reusability of the microgels (Running buffer: pH 7.0 phosphate; temperature: 25 °C; initial DNA concentration: 0.5 mg/mL)

iciency and so on [47,48]. After five uses, it was found that the reduction was only 10% of the initial adsorption capacity, resulting a good recycling ability compared with the earlier studies [35,38,49].

CONCLUSION

In the microholes of a microstencil array chip, poly(2-hydroxyethyl methacrylate-co-glycidyl methacrylate) microgels were created by free radical polymerization in the presence of N,N'-methylenebisacrylamide as a crosslinker. Then, adenine was immobilized to microgels using glycidyl methacrylate's epoxy groups. At a DNA concentration of around 2.0 mg/mL, the amount of DNA adsorbed onto the microgels reached a saturation level after initially growing. The amount of adsorbed DNA apparently depends on the initial DNA concentration. At the optimal temperature and pH of the medium, the maximum adsorption was 20.18 mg/g and 38.54 mg/g microgels at initial DNA concentrations of 0.5 and 2.0 mg/mL, respectively. It has been demonstrated that DNA adsorption capacity was not noticeably decreased throughout repeated adsorption-desorption cycles. This study showed that adsorption materials of desired size, shape, and uniform size can be easily produced using the microfabrication technique.

CONFLICT OF INTEREST

Authors approve that to the best of their knowledge, there is not any conflict of interest or common interest with an institution/organization or a person that may affect the review process of the paper.

AUTHOR CONTRIBUTION

Kemal Cetin Methodology, Investigation, Visualization, Writing - original draft.

REFERENCES

- Chen XW, Mao QX, Liu JW, Wang JH. Isolation/separation of plasmid DNA using hemoglobin modified magnetic nanocomposites as solid-phase adsorbent. *Talanta* 2012;100:107–12.
- Fakurpur Shirejini S, Dehnavi SM, Jahanfar M. Potential of superparamagnetic iron oxide nanoparticles coated with carbon dots as a magnetic nanoadsorbent for DNA isolation. *Chem Eng Res Des* 2023;190:580–9.
- Türkcan C, Akgöl S, Denizli A. Silanized polymeric nanoparticles for DNA isolation. *Mater Sci Eng C* 2013;33:4498–503.
- Akrami M, Dehnavi SM, Barjasteh M, Jahanfar M. Synthesis and characterization of iron oxide/functionalized graphene oxide nanocomposites for highly efficient DNA isolation. *Mater Sci Eng B* 2023;292:116401.
- Erol K. DNA adsorption via Co(II) immobilized cryogels. *J*

- Macromol Sci Part A 2016;53:629-35.
6. Akgönüllü S, Denizli A. Recent advances in optical biosensing approaches for biomarkers detection. *Biosens Bioelectron X* 2022;12:100269.
 7. Köse K. Nucleotide incorporated magnetic microparticles for isolation of DNA. *Process Biochem* 2016;51:1644-9.
 8. Çetin K. Metal-Ion Assisted Imprinted Hydrogels For Recognition Of Lysozyme. *Duzce Univ J Sci Technol* 2021;9:545-55.
 9. Şarkaya K, Yildirim M, Alli A. One-step preparation of poly(NIPAM-pyrrole) electroconductive composite hydrogel and its dielectric properties. *J Appl Polym Sci* 2021;138:50527.
 10. Gopinathan J, Noh I. Click Chemistry-Based Injectable Hydrogels and Bioprinting Inks for Tissue Engineering Applications. *Tissue Eng Regen Med* 2018 155 2018;15:531-46.
 11. Rizzo F, Kehr NS. Recent Advances in Injectable Hydrogels for Controlled and Local Drug Delivery. *Adv Healthc Mater* 2021;10:2001341.
 12. Yang YJ, Mai DJ, Dursch TJ, Olsen BD. Nucleopore-Inspired Polymer Hydrogels for Selective Biomolecular Transport. *Biomacromolecules* 2018;19:3905-16.
 13. Grayson ACR, Shawgo RS, Johnson AM, Flynn NT, Li Y, Cima MJ, vd. A BioMEMS review: MEMS technology for physiologically integrated devices. *Proc IEEE* 2004;92:6-21.
 14. Chován T, Guttman A. Microfabricated devices in biotechnology and biochemical processing. *Trends Biotechnol* 2002;20:116-22.
 15. Sohn LL, Schwille P, Hierlemann A, Tay S, Samitier J, Fu J, vd. How Can Microfluidic and Microfabrication Approaches Make Experiments More Physiologically Relevant *Cell Syst* 2020;11:209
 16. Chung BG, Lee KH, Khademhosseini A, Lee SH. Microfluidic fabrication of microengineered hydrogels and their application in tissue engineering. *Lab Chip* 2011;12:45-59.
 17. Yanagawa F, Sugiura S, Kanamori T. Hydrogel microfabrication technology toward three dimensional tissue engineering. *Regen Ther* 2016;3:45-57.
 18. Coutinho DF, Sant S, Shakiba M, Wang B, Gomes ME, Neves NM, vd. Microfabricated photocrosslinkable polyelectrolyte-complex of chitosan and methacrylated gellan gum. *J Mater Chem* 2012;22:17262-71.
 19. Robert Walker T, Wu L, Patel K, Zandieh M, Liu J. Promotion of DNA Adsorption onto Microplastics by Transition Metal Ions. *Microplastics* 2023, Vol 2, Pages 158-167 2023;2:158-67.
 20. Wang X, Fei W, Zhou Z, Zhu M, Chang Y, Guo Q, vd. Immobilization of Multivalent Titanium Cations on Magnetic Composite Microspheres for Highly Efficient DNA Extraction and Amplification. *ACS Appl Mater Interfaces* 2023;15:42170-81.
 21. Çorman ME, Bereli N, Özkara S, Uzun L, Denizli A. Hydrophobic cryogels for DNA adsorption: Effect of embedding of monosize microbeads into cryogel network on their adsorptive performances. *Biomed Chromatogr* 2013;27:1524-31.
 22. Zandieh M, Patel K, Liu J. Adsorption of Linear and Spherical DNA Oligonucleotides onto Microplastics. *Langmuir* 2022;38:1915-22.
 23. Wang J, Wang Z, Huang PJJ, Bai F, Liu J. Adsorption of DNA Oligonucleotides by Self-Assembled Metalloporphyrin Nanomaterials. *Langmuir* 2022;38:3553-60.
 24. Meng Y, Liu P, Zhou W, Ding J, Liu J. Bioorthogonal DNA Adsorption on Polydopamine Nanoparticles Mediated by Metal Coordination for Highly Robust Sensing in Serum and Living Cells. *ACS Nano* 2018;12:9070-80.
 25. Muñoz ADO, Escobedo-Morales A, Skakerzadeh E, Anoto EC. Effect of homonuclear boron bonds in the adsorption of DNA nucleobases on boron nitride nanosheets. *J Mol Liq* 2021;322:114951.
 26. Memmedova T, Armutcu C, Uzun L, Denizli A. Polyglycidyl methacrylate based immunoaffinity cryogels for insulin adsorption. *Mater Sci Eng C* 2015;52:178-85.
 27. Yoshikawa T, Umeno D, Saito K, Sugo T. High-performance collection of palladium ions in acidic media using nucleic-acid-base-immobilized porous hollow-fiber membranes. *J Memb Sci* 2008;307:82-7.
 28. Çetin K, Denizli A. Polyethylenimine-functionalized microcryogels for controlled release of diclofenac sodium. *React Funct Polym* 2022;170:105125.
 29. Zhang D, Domke KF, Pettinger B, Zhang D, Domke KF, Pettinger B. Tip-Enhanced Raman Spectroscopic Studies of the Hydrogen Bonding between Adenine and Thymine Adsorbed on Au (111). *ChemPhysChem* 2010;11:1662-5.
 30. Ullah F, Othman MBH, Javed F, Ahmad Z, Akil HM. Classification, processing and application of hydrogels: A review. *Mater Sci Eng C* 2015;57:414-33.
 31. Üzek R, Uzun L, Şenel S, Denizli A. Nanospines incorporation into the structure of the hydrophobic cryogels via novel cryogelation method: An alternative sorbent for plasmid DNA purification. *Colloids Surfaces B Biointerfaces* 2013;102:243-50.
 32. Zandieh M, Liu J. Transition Metal-Mediated DNA Adsorption on Polydopamine Nanoparticles. *Langmuir* 2020;36:3260-7.
 33. Tanaka T, Sakai R, Kobayashi R, Hatakeyama K, Matsunaga T. Contributions of phosphate to DNA adsorption/desorption behaviors on aminosilane-modified magnetic nanoparticles. *Langmuir* 2009;25:2956-61.
 34. Zhang HP, Bai S, Xu L, Sun Y. Fabrication of mono-sized magnetic anion exchange beads for plasmid DNA purification. *J Chromatogr B* 2009;877:127-33.
 35. Perçin I, Sağlar E, Yavuz H, Aksöz E, Denizli A. Poly(hydroxyethyl methacrylate) based affinity cryogel for plasmid DNA purification. *Int J Biol Macromol* 2011;48:577-82.
 36. Chiang CL, Sung CS, Chen CY. Application of silica-magnetite nanocomposites to the isolation of ultrapure plasmid DNA from bacterial cells. *J Magn Magn Mater* 2006;305:483-90.
 37. Ongkudon CM, Danquah MK. Anion exchange chromatography of 4.2 kbp plasmid based vaccine (pcDNA3F) from alkaline lysed E. coli lysate using amino functionalised polymethacrylate conical monolith. *Sep Purif Technol* 2011;78:303-10.
 38. Çimen D, Yılmaz F, Perçin I, Türkmen D, Denizli A. Dye affinity cryogels for plasmid DNA purification. *Mater Sci Eng C* 2015;56:318-24.
 39. Saraji M, Yousefi S, Talebi M. Plasmid DNA purification by zirconia magnetic nanocomposite. *Anal Biochem* 2017;539:33-8.
 40. Medina-Llamas JC, Chávez-Guajardo AE, Andrade CAS, Alves KGB, de Melo CP. Use of magnetic polyaniline/maghemite nanocomposite for DNA retrieval from aqueous solutions. *J Colloid Interface Sci* 2014;434:167-74.
 41. Önal B, Odabaşı M. Design and application of a newly generated bio/synthetic cryogel column for DNA capturing. *Polym Bull* 2021;78:6011-28.
 42. Ceylan Ş, Kalburcu T, Gedikli M, Odabaşı M. Application of Cu²⁺-attached Magnetite Nanoparticles Embedded Supermacroporous Monolithic Composite Cryogels for DNA Adsorption. *Hacettepe J Biol Chem* 2011;39:163-72.
 43. Han Y, Forde GM. Single step purification of plasmid DNA using peptide ligand affinity chromatography. *J Chromatogr B* 2008;874:21-6.
 44. Liu B, Liu J. DNA adsorption by indium tin oxide nanoparticles. *Langmuir* 2015;31:371-7.
 45. Li X, Zhang J, Gu H. Adsorption and desorption behaviors of DNA with magnetic mesoporous silica nanoparticles. *Langmuir*

- 2011;27:6099–106.
46. Çetin K. Magnetic nanoparticles embedded microcryogels for bilirubin removal. *Process Biochem* 2022;112:203–8.
 47. Altaf R, Lin X, Zhuang W qin, Lu H, Rout PR, Liu D. Nitrotrismethylenephosphonate sorption from wastewater on zirconium-lanthanum modified magnetite: Reusability and mechanism study. *J Clean Prod* 2021;314:128045.
 48. Suresh Kumar P, Ejerssa WW, Wegener CC, Korving L, Dugulan AI, Temmink H, vd. Understanding and improving the reusability of phosphate adsorbents for wastewater effluent polishing. *Water Res* 2018;145:365–74.
 49. Bhar R, Kanwar R, Mehta SK. Surface engineering of nanoparticles anchored meso-macroporous silica heterostructure: An efficient adsorbent for DNA. *Mater Chem Phys* 2020;255:123541.